# Compressive behaviour of a squeeze cast AJ50 magnesium alloy

**Z. Trojanová\*, Z. Drozd, P. Lukáč**

Department of Physics of Materials, Faculty Mathematics and Physics,
Prague, Ke Karlovu 5, CZ-121 16 Praha 2, Czech Republic
* Corresponding author: E-mail address: ztrojan@met.mff.cuni.cz

### Properties

## ABSTRACT

**Purpose:** There is very limited information about the mechanical properties of Mg-Al-Sr alloys and therefore it is important to investigate mechanical properties at different temperatures and to estimate the mechanisms responsible for the deformation behaviour of Mg-Al-Sr alloys at elevated temperatures.

**Design/methodology/approach:** Deformation behaviour of a Mg-Al-Sr magnesium alloy has been studied in compression in the temperature interval from room temperature up to 300 °C. Stress relaxation tests were performed with the aim to find parameters of the thermally activated process.

**Findings:** The yield stress as well as the maximum stress of the alloy are very sensitive to the testing temperature. Analysis of the work hardening coefficient determined the hardening and softening mechanisms operating during the deformation.

**Practical implications:** The estimated activation energy and values of the activation volume indicate that the main thermally activated process is very probably the glide of dislocations in the non-compact planes.

**Originality/value:** An analysis showed that the main hardening process is the storage of dislocations at impenetrable obstacles. The activation volume values indicate that the main thermally activated process is connected with recovery process.

**Keywords:** Mechanical properties; Magnesium alloy; Stress relaxation; Hardening; Thermal activation

## 1. Introduction

Magnesium alloys are, in the recent years, used to an increasing extent in applications where the components are subjected to elevated temperatures [1-5]. The mechanical properties of magnesium alloys are widely influenced by alloying elements and the thermal treatment. New Mg-Al-Sr alloys are being developed with the aim to find cast alloys with good creep resistance and good strength and replace expensive rare earth alloying elements with some cheaper ones. M. Pekguleryuz [6] reported that Mg-Al-Sr alloys show different microstructures based on the Sr/Al ratio. For Sr/Al ratio below about 0.3, only the $Al_4Sr$ intermetallic phase is the second phase in the structure. When the Sr/Al ratio is higher, a second intermetallic phase, a new ternary Mg-Al-Sr compound, is observed. When the Sr/Al ratio is very low, there is insufficient amount of Sr to bind all Al

atoms and the excess Al would form the $Mg_{17}Al_{12}$ phase. These conclusions were confirmed by Parvez et al. [7] who investigated 22 alloys from the Mg-Al-Sr system.

There is very limited information about the mechanical properties of Mg-Al-Sr alloys and therefore it is important to investigate mechanical properties at different temperatures and to estimate the mechanisms responsible for the deformation behaviour of Mg-Al-Sr alloys at elevated temperatures.

## 2. Experimental procedure

The AJ50 magnesium alloy (nominal composition in w%: 5Al-0.6Sr-balance Mg) used in this study was prepared by the squeeze cast technique. Samples for compression tests with dimensions of 5x5x10 $mm^3$ were deformed in an Instron testing

Short paper

**47**

machine at an initial strain rate of $8 \times 10^{-5}$ s$^{-1}$. The temperature in the furnace was maintained with an accuracy of ±1°C. Sequential stress relaxation (SR) tests were performed at increasing stress (strain) along a stress-strain curve. Duration of the SR was 300 s.

## 3. Experimental results

Figure 1 shows optical micrograph of the as cast alloy. The primary Mg grains are surrounded by the interconnected network of the grain boundary phase. This phase is formed during solidification process and it has lamellar type morphology.
The γ phase ($Mg_{17}Al_{12}$) is also visible. $Al_4Sr$ phase with lamellar eutectic morphology is similar to that found in [3] for alloy with similar composition.
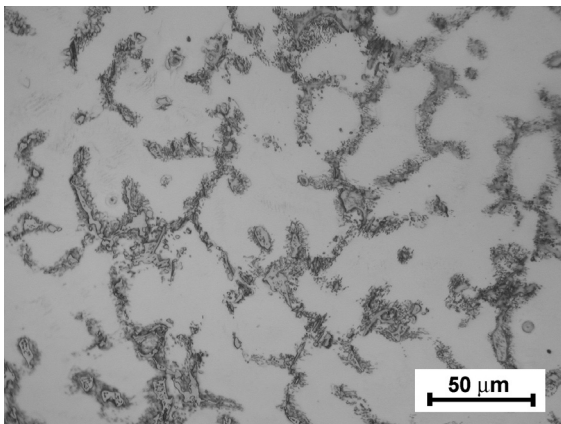


Fig. 1. Microstructure of the as cast alloy

The flow curves are introduced in Fig. 2 for various temperatures. Samples were deformed either to failure or the tests performed at temperatures higher than 100 °C were interrupted at a predetermined strain.
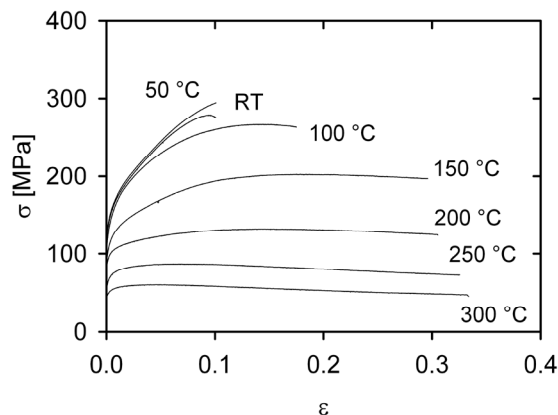


Fig. 2. Stress-strain curves for various temperatures

Fig. 3 shows the temperature dependence of the yield stress as well as the maximum stress. The characteristic stresses decrease

with increasing temperature for T > 50 °C. In a stress relaxation test, the specimen is deformed to a certain stress $\sigma_0$ and then the machine is stopped and the stress is allowed to relax. The stress decreases with time t. The specimen can be again reloaded and deformed to a higher stress (strain) and the stress relaxation test may be repeated.
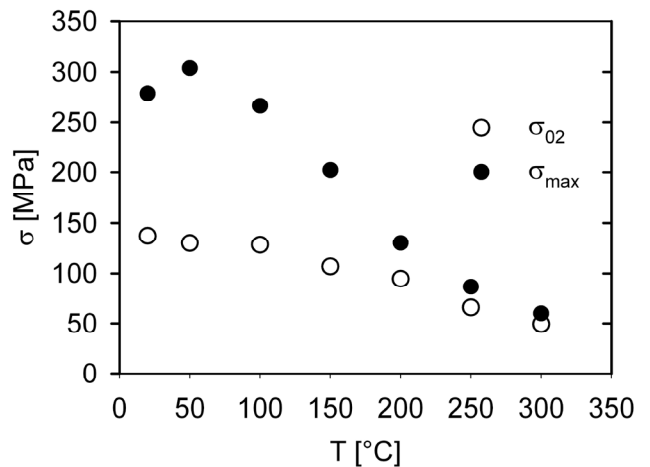


Fig. 3. Temperature dependences of characteristic stresses

## 4. Discussion

### 4.1. Strain hardening

It is widely accepted that the resolved shear stress τ necessary for the dislocation motion in the slip plane can be divided into two components:

$$\tau = \tau_i + \tau^*, \tag{1}$$

where $\tau_i$ is the (internal) athermal contribution to the stress, resulting from long-range internal stresses impeding the plastic flow;

$$\tau_i = \alpha_1 Gb\rho_t^{1/2}, \tag{2}$$

where G is the shear modulus, $\alpha_1$ is a constant describing interaction between dislocations, b is the Burgers vector of dislocations and $\rho_t$ is the total dislocation density. The effective shear stress τ* acts on dislocations during their thermally activated motion when they overcome short range obstacles. The dislocation velocity (the plastic shear strain rate) is controlled by obstacles (their strength, density) and it depends on temperature and the effective shear stress. In polycrystalline materials, the resolved shear stress τ and its components are related to the applied stress σ and its corresponding components by the Taylor orientation factor ψ: $\sigma = \psi\tau$. The flow stress, σ, of ductile metals depends on the average dislocation density, $\rho_t$, as $\sigma \propto \sqrt{\rho_t}$. The dislocation structure evolves with plastic deformation. Dislocations stored at the obstacles contribute to hardening while processes such as cross slip and climb of dislocations contribute to softening. Dislocations after cross slip and/or climb may

annihilate, which causes a decrease in the work hardening rate $\Theta = (\partial\sigma / \partial\varepsilon)_{\dot{\varepsilon},T}$ (where $\varepsilon$ is the true plastic strain and T is the temperature), usually observed at large applied stresses and strains [8, 9].

Lukáč and Balík [8] divide their evolution equation of dislocation density into two hardening and two softening components. They assume that the hardening occurs due to the multiplication of dislocations at both impenetrable obstacles and forest dislocations. Annihilation of dislocations, due to cross slip and/or dislocation climb, is considered as the dominant softening process. The stress dependence of the work hardening rate for polycrystals can thus be written in the form:

$$\Theta = A/(\sigma - \sigma_y) + B - C(\sigma - \sigma_y) - D(\sigma - \sigma_y)^3 , \qquad (3)$$

where the parameter A is connected with the interaction of dislocations with the non-dislocation obstacles and is expected to increase with increasing solute content or the presence of precipitates of second phase particles; the parameter B relates to the work hardening due to the interaction with forest dislocations; the parameter C relates to recovery due to cross slip; the parameter D is connected with climb of dislocations and $\sigma_y$ is the applied yield stress. Analysis of the work hardening rate according to eq. (3) gives the values of the model parameters introduced in Table 1. It should be mentioned that the Lukáč and Balík model describes reasonably the experimentally estimated stress dependence of the work hardening rate only at temperatures up to 200 °C.

Table 1.
Parameters of the tested model

|  | 25°C | 50°C | 100°C | 150°C | 200°C |
|---|---|---|---|---|---|
| $\sigma_y$ (MPa) | 124.0 | 116.0 | 108.0 | 94.4 | 88 |
| A (MPa$^2$) | 105000 | 125000 | 176000 | 753000 | 15900 |
| B (MPa) | 742 | 630 | 454 | 20 | 5.7 |
| C | 3.07 | 2.98 | 8.14 | 4.70 | 7.47 |
| D (MPa$^{-2}$) | 4.94e-9 | 2.43e-8 | 4.81e-8 | 2.00e-4 | 8.46e-9 |
| $\sigma_{02}$ (MPa) | 123.8 | 132 | 123.5 | 96.5 | 82.2 |

From the Table 1 it follows that the main obstacles remain the impenetrable obstacles. The development of the dislocation density increases the storage probability of dislocations. This could cause the temperature decrease in the parameter B, which is really observed. The parameter C increases with temperature, which indicates that cross slip becomes a significant recovery process at higher temperatures. The parameter $D$ increases with increasing temperature, which is expected in the case of climb. Above 200 °C, the model does not describe the experimental curves satisfactory. A decrease in the forest dislocation density (the density of dislocations in non-basal planes) can be expected with increasing temperature.

## 4.2. Thermal activation

Components of the applied stress ($\sigma_i$, $\sigma^*$) were estimated using Li's method [11]. The SR curves were fitted to the power law function in the form: $\sigma - \sigma_i = [a\,(m-1)]^{\frac{1}{1-m}}(t + t_0)^{\frac{1}{1-m}}$, where a, $t_0$ and m are fitting parameters. The time derivative $\dot{\sigma} = d\sigma/dt$ is the stress relaxation rate and $\sigma = \sigma(t)$ is the flow stress at time t during the SR. Stress relaxation tests are very often analysed under the assumption that the stress relaxation rate is proportional to the strain rate $\dot{\varepsilon}$ according to [12] as:

$$\dot{\varepsilon} = -\dot{\sigma}/M \qquad (4)$$

where M is the combined modulus of the specimen – machine set. Considering that the SR is thermally activated dislocation motion through the field of local obstacles, the mean velocity of dislocations is connected with the strain rate by the Orowan equation

$$\dot{\varepsilon} = (1/\psi)\rho\,b\,v \qquad (5)$$

where v is the mean dislocation velocity. It is obvious that the stress dependence of $\dot{\varepsilon}$ is done by the stress dependence of $\rho$ and v. At finite temperature, the obstacles can be overcome with the help of thermal fluctuation. If a single process is controlling the rate of dislocation glide, the plastic strain rate $\dot{\varepsilon}$ can be expressed as:

$$\dot{\varepsilon} = \dot{\varepsilon}_0 \exp\left[-\frac{\Delta G(\sigma^*)}{kT}\right] \qquad (6)$$

where $\dot{\varepsilon}_0$ is a pre-exponential factor containing the dislocation density, the average area covered by the dislocations in every activation act, the Burgers vector, the vibration frequency, and the geometric factor. $\Delta G(\sigma^*)$ is the change of Gibbs free enthalpy depending on the effective stress $\sigma^*$, k is the Boltzmann constant and T is the absolute temperature. The stress dependence of the Gibbs free enthalpy my be expressed by a simple relation

$$\Delta G(\sigma^*) = \Delta G_0 - V\sigma^*, \qquad (7)$$

where $\Delta G_0$ is the Gibbs free energy (called the barrier activation energy) in the absence of stress and V is the activation volume. The nature and the distribution of obstacles determine the activation parameters (the activation energy and the activation volume). For a given arrangement of obstacles in a material, the thermally activated process determines the temperature and strain rate dependence of the flow stress. The activation energy $\Delta G_0$ and the activation volume V are needed to identify the thermally activated mechanism. Combining (6), (8) and (9), we have

$$-\dot{\sigma} = M\dot{\varepsilon}_0 \exp\left[-\frac{\Delta G_0 - V\sigma^*}{kT}\right] \qquad (8)$$

Taking the logarithm of this equation we get

$$\ln(-\dot{\sigma}) = \ln(M\dot{\varepsilon}_0) - \frac{\Delta G_0}{kT} + \frac{V\sigma^*}{kT} \qquad (9)$$

Integration of (11) results to the known Feltham equation [12]

$$\Delta\sigma(t) = \sigma(0) - \sigma(t) = \alpha\ln(\beta t + 1) \qquad (10)$$

where $\sigma(0)$ is the stress at the beginning of stress relaxation at time t = 0,

$$\alpha = kT/V \qquad (11)$$

$$\beta = \frac{M\dot{\varepsilon}_0 V}{kT}\exp\left[-\frac{\Delta G_0 - V\sigma^*(0)}{kT}\right] = \frac{M\dot{\varepsilon}(0)}{\alpha} \qquad (12)$$

where $\dot{\varepsilon}(0)$ the plastic strain rate at the beginning of the relaxation. The activation volumes $V_{app}$ for AJ50 magnesium alloy polycrystals were estimated using equations (10) and (11). As usual, the values of V divided by $b^3$ are plotted against the effective stress $\sigma^*$ for three testing temperatures in Figure 4. It

can be seen that the activation volumes decrease with σ* for all tested temperatures. It is seen that the values of the activation volume lie on one line - "master curve"
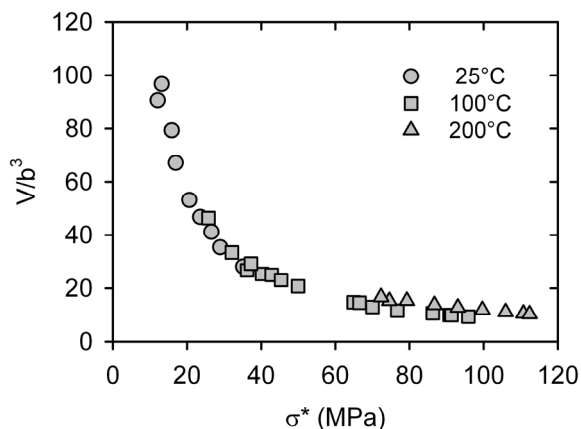


Fig. 4. The plot of the activation volume in $b^3$ against the thermal stress σ* for various temperatures

The activation enthalpy calculated for 100 °C gives (1.00 ± 0.05) eV. The main thermally activated process has connection with the dynamic recovery. Kocks et al. [14] suggested an empirical equation between the Gibbs enthalpy ΔG and the effective stress σ* in the following form:

$$\Delta G = \Delta G_0 \left[ 1 - \left( \frac{\sigma^*}{\sigma_0^*} \right)^p \right]^q \tag{13}$$

where $\Delta G_0$ and $\sigma_0^*$ are Gibbs enthalpy and the effective stress at 0 K. For the effective stress it follows:

$$\sigma^* = \sigma_0^* \left[ 1 - \left( \frac{kT}{\Delta G_0} \ln \frac{\dot{\varepsilon}_0}{\dot{\varepsilon}} \right)^{1/q} \right]^{1/p} \tag{14}$$

where p and q are phenomenological parameters reflecting the shape of a resistance obstacle profile [15] . Activation volume is done by the equation

$$V = \frac{\Delta G_0 pq}{\sigma_0^*} \left[ 1 - \left( \frac{\sigma^*}{\sigma_0^*} \right)^p \right]^{q-1} \left( \frac{\sigma^*}{\sigma_0^*} \right)^{p-1} \tag{15}$$

The values of the activation volume should lie at the curve given by the equation (15).

## 5. Conclusions

The deformation behaviour of the AJ50 magnesium alloy has been studied in compression over the temperature range from room temperature to 300 °C. An analysis showed that the main hardening process is the storage of dislocations at impenetrable obstacles. The activation volume depends on the effective stress so that all values lie on the master curve. The estimated activation energy and values of the activation volume indicate that the main

thermally activated process is very probably the glide of dislocations in the non-compact planes.

## Acknowledgements

## References

[1] M. Pahutová, V. Sklenička, K. Kuchařová, M. Svoboda, Creep resistance of magnesium alloys and their composites, International Journal of Materials & Product Technology 18 (2003) 116-140.

[2] Z. Trojanová, P. Lukáč, Compressive deformation behavior of magnesium alloys, Journal of Materials Processing Technology 162-163 (2005) 416-421.

[3] M.S. Yong, A.J. Clegg, Process optimisation for a squeeze cast magnesium alloy, Journal of Materials Processing Technology 145 (2004) 134-141.

[4] A. Kiełbus, Structure and machanical properties of casting MSR-B magnesium alloy, Journal of Achievements in Materials and Manufacturing Engineering 18 (2006) 131-134.

[5] A. Kiełbus, Microstructure of AE44 magnesium alloy before and after hot chamber die casting, Journal of Achievements in Materials and Manufacturing Engineering 20 (2007) 459-462.

[6] M. Pekguleryuz, Creep resistant magnesium alloys for power-train applications, Magnesium Alloys and Their Applications (Ed. K.U. Kainer), DGM, Willey-VCH 2003, 65-85.

[7] M.A. Parvez, M. Medraj, E. Essadiqi, A. Muntasar, G. Dénès, Experimental study of the ternary magnesium–aluminium–strontium system, Journal of Alloys and Compounds 402 (2005) 170-185.

[8] U.F. Kocks, Laws for work hardening and low temperature creep, Journal of Engineering Materaterials and Technology 98 (1976) 76-85.

[9] Y. Estrin, H. Mecking, A unified phenomenological description of work hardening and creep based on one-parameter models, Acta Metallurgica 32 (1984) 57-70.

[10] P. Lukáč, J. Balík, Kinetics of plastic deformation, Key Engineering Materials, 97-98 (1994) 307-322.

[11] J.C.M. Li, Dislocation Dynamics in Deformation and Recovery, Canadian Journal of Applied Physics 45 (1967) 493-509.

[12] M. Hamerský, Z. Trojanová, P. Lukáč, Stress relaxation in metallic polycrystals, Acta Technica ČSAV 37 (1992) 263-292.

[13] P. Feltham, Stress relaxation in magnesium at low temperatures, Physica Status Solidi 3 (1963) 1340-1346.

[14] U.F. Kocks, A.S. Argon, M.F. Ashby, Thermodynamics and Kinetics of Slip, Progress in Materials Science 19 (1975) 1- 288.

[15] K. Ono, Temperature dependence of dispersed barrier hardening. Journal of Applied Physics 39 (1968) 1803-1806.